Single- and Multi-Correlator Sequential Tests for Signal Integrity in Multi-Antenna GNSS Receivers

Daniel Egea, Gonzalo Seco-Granados, José A. López-Salcedo
Department of Telecommunications and Systems Engineering
Universitat Autònoma de Barcelona (UAB)
Bellaterra 08193, Barcelona (Spain)

***Abstract*—Multipath mitigation has attracted the attention of many researchers, thus leading to outstanding contributions in the past years. In contrast, multipath *detection* has not benefited that much. It has remained in background, with most of the current state of the art still relying on classical detection techniques. In this paper, we take a leap forward in multipath detection, and we propose a CUSUM-based sequential change detection algorithm. The aim is to focus on quickest detection techniques in order to detect the presence of multipath and to provide integrity to GNSS receivers. We will focus herein on multi-antenna GNSS receivers, with both single and multi correlator architectures, and numerical results will be used to validate the proposed technique.**

I. Introduction

With the widespread deployment of Global Navigation Satellite Systems (GNSS), one of the major challenges to be solved is the provision of integrity to users beyond the civil aviation community, where this feature is already a well-established performance criterion [1]. *Integrity* refers to the ability of the user receiver to guarantee the quality and trust of the received signal, in such a way that critical or commercial applications can be safely operated.

Position integrity is typically provided in civil aviation by Receiver Autonomous Integrity Monitoring (RAIM) algorithms and Satellite Based Augmentation Systems (SBAS). However, such methods need requirements that cannot be fulfilled in road and urban environments, due to effects like multipath, Non-Line-Of-Sight (NLOS) propagation and interference signals. This implies that the signal integrity, which in civil aviation is almost translated into position integrity, can hardly be used to ensure position integrity in terrestrial environments [2]. It is for this reason that signal integrity is actually a concern within the GNSS community, motivated by the widespread deployment of terrestrial GNSS receivers and the emergence of new GNSS-based applications and services [3].

In this paper, we will concentrate on multipath and NLOS as the major impairments that can threat the integrity of mass-market users (mainly, those using GNSS receivers in urban environments). Significant efforts have been made to mitigate multipath effects, often leaving multipath detection in background. However, multipath detection is actually as important, or even more important than multipath mitigation. The reason is that before using mitigation techniques, we need to know whether multipath is present or not. Otherwise, the effects of mitigation techniques could seriously damage the GNSS signal of interest. Most existing multipath detection methods operate at observable level, such as [4] which is based on pseudoranges and carrier phase measurements, or [5], [6], where map models are used to describe potential environment obstacles of causing multipath reflections.

Methods at observable level are not able to cope with short multipath delays, and those using maps need prior information about the user environment. Unfortunately, close multipath cannot be ignored from an integrity point of view, since it strongly affects GNSS signals. Moreover, we cannot rely on having access to external information, such as map models, since this information is not always available. Consequently, there is a need of stand-alone multipath detectors in order to provide flexibility, control, and reliability in handling multipath, even with short delays.

Recently, this kind of detectors have been addressed in [7] and [8]. These contributions adopt a classic detection framework, in which the goal is to minimize the miss probability (or maximize the detection probability) subject to constrains on the false alarm rate. A common feature of these schemes is that the detection is carried out in a block-wise manner, where a batch of samples is processed at a time. In this paper, we adopt an alternative point of view of the detection problem. Besides detection probability, detection delay is also a critical performance metric for integrity monitoring purposes, since a small detection delay will allow to detect quickly the threats. Focusing on the detection delay, we will be able to provide a level of signal integrity that could not be achieved by means of classical detection techniques. Obviously, the desire to reduce the detection delay must be balanced with a certain false alarm constraint.

The quickest detection framework has been extensively studied in the past decades. One of the most popular techniques is the CUSUM algorithm [9], which is a sequential method aimed at minimizing the detection delay subject to a false alarm constraint. The CUSUM algorithm has been applied to automatic control since a long time ago, and more recently, to multi-antenna receivers for signal detection [10], and to spectrum sensing in cognitive radio [11]. Nevertheless, to the best of the authors' knowledge, the CUSUM has not been used yet for multipath detection and GNSS integrity monitoring.

Based on this observation, the goal of this work is to bridge the gap between quickest detection theory and multipath detection methods. By doing so, we will able to provide a sequential detection framework for multipath detection with aim of improving the GNSS integrity. In [12] a multipath detection method for a single-correlation multi-antenna GNSS receiver was proposed. This work moves one step further and considers multi-correlation multi-antenna schemes, thus covering both possibilities of GNSS receiver architectures.

The rest of this paper is organized as follows. Section II introduces the signal model and Section III describes the CUSUM algorithm and the proposed metrics for multipath detection. In Section IV, numerical results are presented to evaluate the proposed detection techniques and compare them with present multipath detection methods. Finally, Section V concludes the paper.

II. Signal Model

Let us consider an antenna array composed of a uniform linear array (ULA) with N_a antenna elements equi-spaced at a distance d. For an incident signal with direction of arrival (DoA) θ, the array

This work was partly supported by the Spanish Government under grant TEC2011-28219 and by the Catalan Government under grant 2009 SGR 298.

978-1-4799-5123-9/14/$31.00 ©2014 IEEE

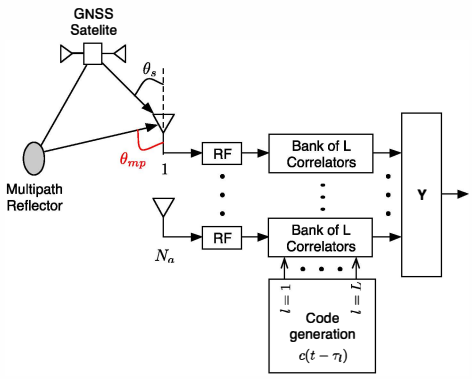

Fig. 1. Scenario representing the presence of multipath in the multi-correlator receiver architecture used in this paper.

response or steering vector has the following form:

$$\mathbf{s}(\theta) = \left[1 \quad e^{j2\pi(d/\lambda)\cos(\theta)} \cdots e^{j(N_a-1)2\pi(d/\lambda)\cos(\theta)}\right]^T \tag{1}$$

where λ is the signal wavelength. The noise at each antenna is modeled as an i.i.d zero-mean complex Gaussian random process with variance σ_w^2, and uncorrelated both spatially and temporally. Fig. 1 shows the situation when a GNSS signal arrives with DoA θ_s at the antenna array and a multipath ray is present with DoA θ_{mp}.

For the multipath detection, the signal processing is carried out at the GNSS receiver correlator output, since it is here where the GNSS signal and multipath effects actually become visible. In this paper, we operate at the output of a bank of correlators with a post detection integration time (PDI), equal to one code period (e.g. 1 ms in the case of GPS L1 C/A signals). We consider a total of L correlation outputs per array arm, which is possible due to the multi-correlation architecture in Fig. 1. With this scheme, the following $(N_a \times L)$ received data matrix can be obtained:

$$\mathbf{Y}_k \doteq [\mathbf{y}(1;k), \cdots, \mathbf{y}(L;k)] \tag{2}$$

where $\mathbf{y}(l;k)$ is the $(N_a \times 1)$ vector with the l-th correlator output at different antennas at the k-th PDI period. Depending on the presence or absence of multipath, the two following hypotheses can be written:

$$\begin{aligned} \mathcal{H}_0 &: \mathbf{y}(l;k) = \alpha_0(l)\cdot\mathbf{s}(\theta_s) + \mathbf{n}(l) \\ \mathcal{H}_1 &: \mathbf{y}(l;k) = \alpha_0(l)\cdot\mathbf{s}(\theta_s) + \alpha_1(l)\cdot\mathbf{s}(\theta_{\text{mp}}) + \mathbf{n}(l) \end{aligned} \tag{3}$$

where the complex amplitude α_j with $j = \{0, 1\}$, corresponds to the LOS and multipath post-correlation outputs components, respectively. Finally, $\mathbf{n}(l;k)$ is the noise vector whose components are the post-correlation zero-mean complex Gaussian noise with variance σ^2. Without loss of generality only one multipath ray is assumed, which is the minimum number of rays needed to differentiate both hypothesis.

Typically, the correlator output samples are taken on either side of the maximum correlation peak. That is to say, the first $(L-1)/2$ correlation samples on the left hand side of the correlation peak correspond to the so-called *early* samples; the correlation sample aligned with the estimated time-delay of the received signal is referred to as the *prompt* sample ($P \doteq (L+1)/2$); and the *late* samples are those corresponding to the last $(L-1)/2$ correlation samples on the right hand side of the correlation peak. This is the case of a multi-correlator receiver architecture, and we will assume that the correlation points are uniformly distributed in the range of ± 1 chip period. For the single-correlator receiver architecture case, a single correlator output sample is available, corresponding to the prompt correlator.

III. Multipath Detection for Integrity Monitoring

A. Fundamentals of quickest detection

For the prompt detection of integrity threats, it is essential to formulate the problem under the framework of online or sequential change detection [9]. To do so, let us first consider a set of K observations $\mathbf{x} \doteq [x(0), x(1), \ldots, x(v), x(v+1), \ldots, x(K-1)]^T$, where v is the time instant at which the multipath appears. Consequently, it is assumed that before v (i.e. at hypothesis $\mathcal{H}_0$) the observation $x(n)$ follows a statistical distribution $f_0(x(n))$ for all $n < v$, whereas after v (i.e. at hypothesis $\mathcal{H}_1$) it follows a different distribution $f_1(x(n))$ for all $n \geqslant v$. Based on these premises, sequential change detection aims at finding the strategy that minimizes the detection delay $\overline{T}_1$, while keeping the mean time between false alarms $\overline{T}_0$ larger than a conveniently set value N_{fa}.

The CUSUM algorithm is a simple but efficient sequential change detection algorithm based on the log likelihood ratio (LLR) of the densities before and after the change [9]. That is, $\text{LLR}(x(n)) \doteq \ln\left(f_1(x(n))/f_0(x(n))\right)$, and it is defined as a decision test comparing the following metric

$$g(n+1) = [g(n) + \text{LLR}(x(n+1))]^+ \tag{4}$$

for some threshold h, where $[x]^+ \doteq \max\{0, x\}$. Hence, it is possible to compute $g(n)$ recursively by setting $g(0) = 0$, and then an alarm is raised whenever $g(n+1) > h$. By doing so, it is known that the CUSUM algorithm minimizes $\overline{T}_1$ among all detection algorithms that satisfy $\overline{T}_0 \geqslant N_{fa}$. The following approximation for $\overline{T}_0$ allows us to find the threshold h that guarantees a given false alarm rate N_{fa}:

$$\overline{T}_0 \geqslant e^h = N_{\text{fa}}. \tag{5}$$

Letting $\text{E}_0[\cdot]$ and $\text{E}_1[\cdot]$ denote the expectation under f_0 and f_1, respectively, the principle underlying (4) is that, before the change, $\text{E}_0[\text{LLR}(x(n))] < 0$, so that $g(n)$ remains close to zero; in contrast, after the change, $g(n)$ starts drifting upward with a positive mean $\text{E}_1[\text{LLR}(x(n))]$ until it ultimately crosses the threshold h.

In general, when the LLR is not completely known (as it is the case in the problem under study), the LLR can be replaced by any other function of the signal samples $x(n)$, $\rho(n) \doteq q(x(n))$, with negative mean before the change, and positive mean after the change. That is,

$$g(n+1) = [g(n) + \rho(n)]^+. \tag{6}$$

In this case, the detection delay is no longer guaranteed to be optimal. Nevertheless, it is still a very good candidate provided that an appropriate function is chosen satisfying the following condition [9]:

$$\overline{T}_0 \geqslant e^{s_0 h} = N_{\text{fa}}, \quad \overline{T}_1 \sim \frac{h}{\text{E}_1[\rho(n)]}. \tag{7}$$

where $s_0 > 0$ is the nonzero root of the equation $\text{E}_0\left[e^{s\cdot\rho(n)}\right] = 1$.

B. Multi-correlation multi-antenna (MC-MA) integrity metric

In order to derive a metric for multipath detection, we will consider the covariance matrix of $\mathbf{Y}_k$, which can be estimated as [13]:

$$\hat{\mathbf{W}} \doteq \text{Cov}[\mathbf{Y}_k] = \hat{\mathbf{R}}_{yy} - \frac{\mathbf{r}_{yc}\mathbf{r}_{yc}^H}{P_c} \tag{8}$$

with the following definitions,

$$\hat{\mathbf{R}}_{yy} \doteq \frac{1}{L}\mathbf{Y}\mathbf{Y}^H \quad \mathbf{r}_{yc} \doteq \frac{1}{L}\mathbf{Y}\mathbf{r}_{cc}^H \tag{9}$$

$$P_c \doteq \frac{1}{L}\mathbf{r}_{cc}\mathbf{r}_{cc}^H \tag{10}$$

and $\mathbf{r}_{cc} \doteq [R_{cc}(\tau_1), \cdots, R_{cc}(\tau_L)]$, where $R_{cc}(\tau_i)$ is the autocorrelation function of the GNSS code evaluated at the time delay τ_i. For the sake of clarity the index k has been omitted, keeping in mind that each data matrix corresponds to a given integration interval.

From [8] it is known that $\hat{\mathbf{W}}$ is a diagonal matrix under $\mathcal{H}_0$, whereas under $\mathcal{H}_1$, it departs from diagonal due to the presence of correlated signals among antenna elements. Thereby, the following test statistic is proposed with the aim of measuring to which extent $\hat{\mathbf{W}}$ departs from a diagonal matrix:

$$\rho_d(k) = 2LN_a \ln \left(\frac{\frac{1}{N_a}\sum_{i=1}^{N_a} \hat{\lambda}_i(k)}{\left[\prod_{i=1}^{N_a} \hat{\lambda}_i(k)\right]^{1/N_a}} \right), \tag{11}$$

where $\hat{\lambda}_i(k)$ is the i-th eigenvalue associated to the estimated covariance matrix $\hat{\mathbf{W}}$ at PDI k. This metric, in the case of a multipath-free scenario, follows a chi-squared distribution with $N_a^2 - 1$ degrees of freedom. Therefore, the following hypothesis testing can be defined:

$$\begin{aligned} \mathcal{H}_0 &: E_0\left[\rho_d(k)\right] = N_a^2 - 1, \\ \mathcal{H}_1 &: E_1\left[\rho_d(k)\right] > N_a^2 - 1. \end{aligned} \tag{12}$$

Note that under $\mathcal{H}_1$ the exact mean is unknown since f_1 is not completely specified (i.e. it depends on the multipath parameters, which will be unknown in practice). Hence, with the aim of being able to use the detection metric $\rho_d(k)$ in the CUSUM algorithm, we propose the following modified metric:

$$\rho_{\mathrm{mc}}(k) \doteq \rho_d(k) - p. \tag{13}$$

In this way, by selecting a proper p, the mean of ρ_{mc} before change will be negative, but it will become positive after the change. Specifically, denoting the mean after change by $\mu_1 > N_a^2 - 1$:

$$\begin{aligned} \mathcal{H}_0 &: \mathrm{E}_0\left[\rho_{\mathrm{mc}}(k)\right] = N_a^2 - 1 - p < 0, \\ \mathcal{H}_1 &: \mathrm{E}_1\left[\rho_{\mathrm{mc}}(k)\right] = \mu_1 - p > 0. \end{aligned} \tag{14}$$

The choice of the offset p should be large enough to assure a negative mean before change and provide a certain false alarm rate (FAR). But at the same time, p should be small enough to fulfill the inequality of hypothesis $\mathcal{H}_1$ in (14) (i.e. to maintain a positive mean after change for the test metric). From (7) and using ρ_{mc} we are able to adjust the FAR through the nonzero root, s_0, of the following equation:

$$\mathrm{E}_0\left[e^{s\cdot\rho_d(k)}\right] e^{-s\cdot p} = 1. \tag{15}$$

We also know that under $\mathcal{H}_0$, $\rho_d(k)$ is a chi-square variable with $N_a^2 - 1$ degrees of freedom. Then, the characteristic function of $\rho_d(k)$ is given by:

$$\mathrm{E}_0\left[e^{s\cdot\rho_d(k)}\right] = (1-2s)^{-\frac{N_a^2-1}{2}} \tag{16}$$

and thus s_0 turns out to be the nonzero root of the following equation:

$$e^{-s\cdot p} = (1-2s)^{\frac{N_a^2-1}{2}} \tag{17}$$

which can be solved numerically. The solution is a function of p and N_a, with the latter being related to the degrees of freedom of the chi-square variable (i.e. $N_a^2 - 1$).

Fig. 2 shows the nonzero root of (17) as a function of the ratio p/N_a^2 for the case of $N_a = 3$. First notice that for $p < N_a^2$, we have $s_0 = 0$ for all p, which is coherent inasmuch as from (14), p must be larger than N_a^2 to get a negative mean under $\mathcal{H}_0$. Next, it is observed that s_0 increases when the bias p is larger than N_a^2,until it reaches a saturation level. Finally, there is a limit on p from which for higher values the above equation does not converge to a numerical solution.

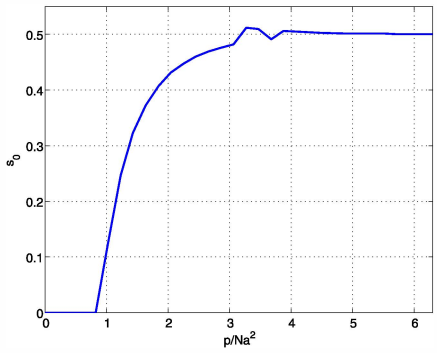

Fig. 2. Nonzero root of (17), s_0, versus the ratio of the bias p between N_a^2.

This value is the limit of the X-axis in Fig. 2, which is around 6.3, and further values are not shown since they do not provide a valid solution. Later on, it will be shown the effects on the FAR of taking p within this region.

C. Single-correlation multi-antenna (SC-MA) integrity metric

For the single-correlation case, we have not enough correlation points to form a precise estimation of the covariance matrix in (8), and thus the proposed detection metric in Section III-B cannot be applied. However, a detection metric for single-correlation receiver architectures is of practical interest, and it will allows us to cover any type of multi-antenna GNSS receiver architecture. To do so, we propose a metric based on the use of the prompt correlator output at each antenna (i.e. $\mathbf{y}(P;k)$), where the contribution of the known DOA of the GNSS signal of interest is removed as follows: $\mathbf{z}(k) \doteq \mathbf{y}(P;k) \odot \mathbf{s}^*(\theta_s)$ with $\odot$ the Schur-Hadamard product.

Thereby, based on $\mathbf{z}(k)$, the following scalar observations are defined to implement the CUSUM algorithm [12]:

$$\rho_{\mathrm{sc}}(k) \doteq \frac{1}{N_a - 1} \sum_{n=2}^{N_a} \left([\mathbf{z}(k)]_n - [\mathbf{z}(k)]_1 \right) \tag{18}$$

where $[\mathbf{z}(k)]_j$ indicates the j-th component of $\mathbf{z}(k)$. This expression denotes the average of the differences between antenna pairs, once the LOS steering vector has been removed. In the absence of multipath, the result is expected to be negligible, since $[\mathbf{z}(k)]_n$ is the same for all antennas. However, in the presence of multipath it contains the different contributions of multipath in different antennas, and thus multipath becomes detectable.

In contrast to [12], the problem is formulated here using complex Gaussian distributions for $\rho_{\mathrm{sc}}(k)$, which avoids the need of two parallel CUSUM algorithms working on the real and imaginary parts of the test metric. As in the case of multi-correlation detection, the distribution at $\mathcal{H}_1$ is not completely known, specifically its mean is unknown. Hence, the solution here is to replace the unknown parameter by its maximum likelihood estimate, leading to the generalized likelihood ratio (GLR) CUSUM algorithm [9]. For a change in the mean of an independent complex Gaussian sequence,which is our case, it leads to:

$$g_{\mathrm{GLR}}(k) = \frac{1}{\sigma_0^2} \max_{1 \leqslant n \leqslant k} \sum_{i=n}^{k} \|\hat{A}_1^n\|^2 + 2\mathbb{R}e\left\{\hat{A}_1^n \cdot \rho_{\mathrm{sc}}^*(k)\right\} \tag{19}$$

with $\hat{A}_1^n \doteq \frac{1}{k-n+1}\sum_{i=n}^{k} \rho_{\mathrm{sc}}(i)$, the maximum likelihood estimate of the complex mean after the change.

Note that to apply the above method, we need to know the DOA of the GNSS signal of interest, θ_s. It is needed in order to

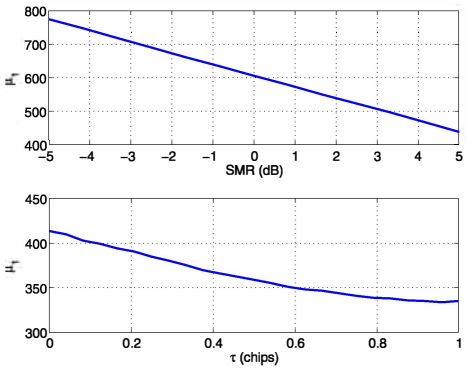

Fig. 3. Sensitivity of μ_1 as a function of SMR at 0.05 chips delay (up) and multipath delay at SMR = 6 dB (down) for C/N0 = 45 dB-Hz.

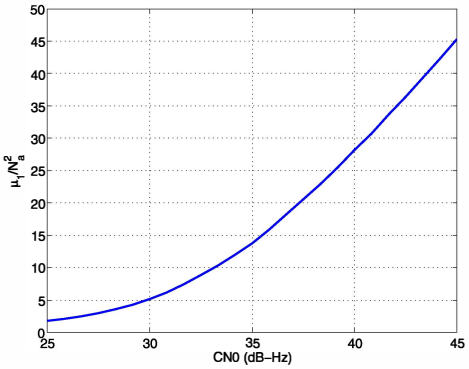

Fig. 4. Sensitivity of μ_1/N_a^2 as a function of C/N_0 with 0.05 chips of multipath delay and $SMR = 6$ dB.

generate $\mathbf{s}^*(\theta_s)$ and compute the vector $\mathbf{z}(k)$ in (18). However, this requirement is feasible in GNSS since the position of visible satellites is already computed within a GNSS receiver. With some further information on the attitude of the receiver, we can obtain the satellite DOA.

IV. Simulation Results

In this section, different experiments are presented with the aim of analyzing the proposed metrics in Section III-B and III-C, and comparing the CUSUM performance with other multipath detection methods available in the literature. To do so, we consider a multi-antenna GNSS receiver with $N_a = 3$ antennas, a precorrelation bandwidth of 2 MHz and a sampling rate of $f_s = 10$ MHz. The integration time is set to PDI $= 1$ ms and a multi-correlator architecture with $L = 37$ correlators is adopted. All experiments consider in-phase LOS and multipath components, with signal DOA $\theta_s = 95°$ and multipath DOA $\theta_{\text{mp}} = 20°$.

A. Experiment 1: Sensitivity of the MC-MA integrity metric.

Fig. 3 shows the variation of the mean at $\mathcal{H}_1$ of the proposed metric in (11) with respect to the signal-to-multipath ratio (SMR) and the relative delay between the LOS signal and the multipath replica. For the SMR variation case, the multipath delay is fixed to $\tau = 0.05$ chips, while for the multipath delay variation, the SMR is fixed to 6 dB. Results show how the value of μ_1 decreases as the SMR or τ_{mp} increase. This is consistent with the fact that multipath effects will be stronger as the SMR or τ_{mp} are lower, and thus μ_1 will increase denoting stronger effects. These results will be different depending on the phase as well as the DOAs of the LOS and multipath replica, becoming difficult to completely characterize the proposed metric when multipath is present. Note that the upper plot of Fig. 3 includes values for negative SMR, which correspond to the NLOS case.

Furthermore, the results in Fig. 4 exhibit a variation of μ_1 with the receiver carrier-to-noise ratio (C/N_0), making more complex the characterization of the metric in presence of multipath. In this case, $\tau = 0.05$ chips and SMR $= 6$ dB. The plot in Fig.4 shows the ratio between μ_1 and N_a^2, which for low C/N_0 takes values around those obtained at $\mathcal{H}_0$ (i.e. $\mu_1 \approx N_a^2 - 1$). This means that for low C/N_0, noise effects are predominant and make difficult to distinguish the presence of multipath at $\mathcal{H}_1$, producing similar results to $\mathcal{H}_0$. For higher C/N_0 values, the ratio μ_1/N_a^2 is around some tens. This behavior allows us to fix a criterion in the choice of the bias term p in (13), since depending on the C/N_0, the difference between the mean after and before the change will be greater or lower.

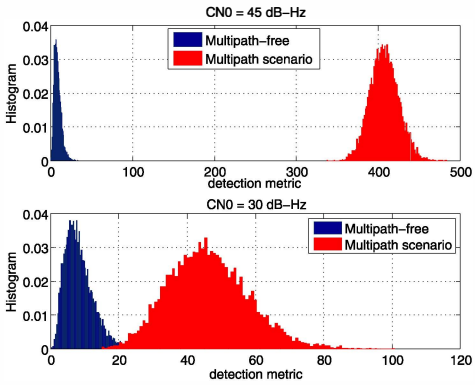

Fig. 5. $\mathcal{H}_0$ and $\mathcal{H}_1$ detection metric histogram for an high C/N_0 (up) and low C/N_0 (down) case.

Fig. 5 shows this behavior and clarifies the idea of choosing the bias term p. In the high C/N_0 case (upper plot), the difference is so large that a large subtracting offset p can be safely used satisfying (14). For instance an appropriate p can be extracted from Fig. 2 as the last valid value for which (17) can be numerically solved (i.e. $p \sim 6.3 \cdot N_a^2 = 56.7$). Using this value, we can see in the upper plot of Fig. 5 that the distributions after and before the change are shifted in such a way that all the values of f_0 and f_1 are below and above 0, respectively, (i.e. a free-FAR region). This behavior allows us to use a sign detector to decide between $\mathcal{H}_0$ and $\mathcal{H}_1$ depending on whether the prompt detection metric is negative or positive, respectively.

On the other hand, for the low C/N_0 case, we cannot use the same value for the bias term because it is too large, leading to $\mu_1 < 0$, and then the CUSUM algorithm would not work. For this reason, as f_1 is unknown, the best way to proceed is by fixing $p = N_a^2$, which is the minimum value to ensure a negative mean before the change according to (14), and it is also small enough to ensure a positive mean after change.

B. Experiment 2: Performance of the MC-MA integrity metric.

Now, we analyze the CUSUM performance using the proposed detection metric ρ_{mc} in (6), and compare it with the performance obtained by using the detection method in [8]. In this case, the precorrelation bandwidth is set to 4 MHz, the multipath delay to $\tau = 0.05$, SMR $= 6$ dB, and low C/N_0 scenarios are simulated in order to provide qualitative results, since for high C/N_0 scenarios we know that the performance will be close to the unity probability

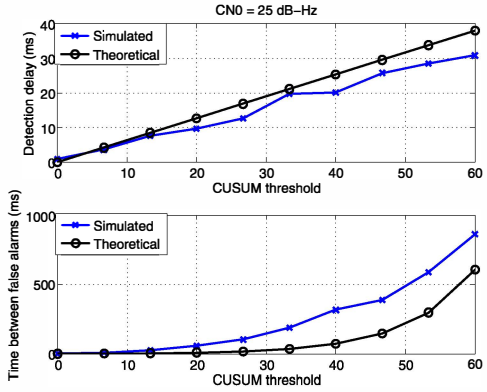

Fig. 6. Multi-correlation method performance as a function of detection threshold h, with a fixed C/N_0 of 25 dB-Hz. Detection delay (up) and time between false alarms(down).

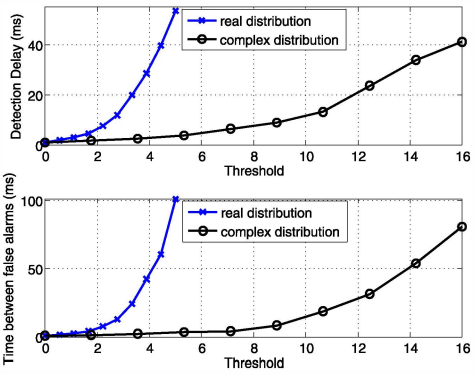

Fig. 8. Single-correlation method performance assuming real and complex distributions. Detection delay (up) and false alarm rate (down).

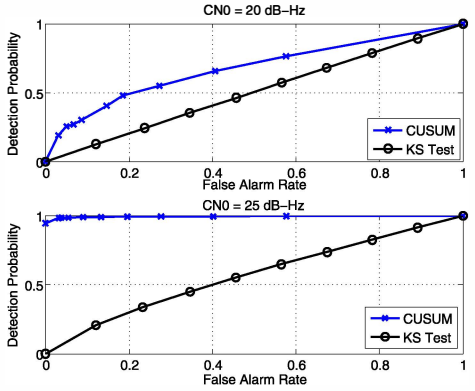

Fig. 7. Simulated ROC comparison between our method and the KS test, applied with $N = 1$, for a $C/N_0 = 20$ dB-Hz (up) and $C/N_0 = 25$ dB-Hz (down).

detection with zero false alarm rate (i.e. free-false alarm rate).

Fig. 6 shows the CUSUM performance fixing $C/N_0 = 25$ dB-Hz, which is compared with the theoretical results in (7). The upper plot represents the detection delay measured in milliseconds with respect the set threshold, and shows similar values for the simulated results and theoretical ones. On the other hand, the lower plot shows how the empirical time between false alarms is greater than the lower bound given in (7), thus it allows us to set a threshold h assuring certain desired FAR N_{fa}.

Next, with the aim of comparing the suggested method with others contributions in the literature, we use the approach in [8] as reference, which is based on the classical Kolmogorov-Smirnov (KS) test. To do a fair comparison between both methods, the block length N used in the KS test must be set to $N = 1$ sample, thereby a decision will be take at each integration period, such as in the proposed method. Moreover, the comparison must be done in terms of detection and false alarm probabilities, since classical detection schemes, as it is the case of KS test, are not designed to be evaluated in terms of detection delay and samples between false alarms.

To do so, we can generate N_s samples from both hypothesis $\mathcal{H}_0$ and $\mathcal{H}_1$ and obtain the probabilities as the ratio of the number of successes at each hypothesis within N_s samples. The number of successes at $\mathcal{H}_0$ and $\mathcal{H}_1$ provide the number of false alarms and detections, respectively. In Fig. 7 it is shown the receiver operating characteristic (ROC) for two different levels of C/N_0. These results confirm the outperforming behavior of the proposed detection method compared to the KS test in the case of a sequential detection ($N = 1$). This is consistent because the KS test, as a classical detection method, is not designed to be optimal in an online detection framework, in contrast of CUSUM which is specifically designed to be optimal in this sense.

Another important observation that can be extracted from Fig. 7 is the difference of performance in the CUSUM algorithm for the case of $C/N_0 = 20$ and 25 dB-Hz. The former produces a mean after the change of the metric in (11) of $\mu_1 = 8.92$, which using a bias offset of $p = N_a^2$ produces a negative value. This value is due to the closeness between densities after and before the change, which is logical as the noise effect prevails the multipath effects, and thus both hypothesis in (3) are very similar. Since this negative value is not very large, the CUSUM algorithm still works and outperforms the KS test. However, the actual power of the proposed method is provided at the lower plot of Fig. 7, which shows how the CUSUM detection probability is near the unity for all false alarm rates. In this case, the mean after the change with $p = N_a^2$ is positive and the CUSUM algorithm works in the standard conditions, which implies a negative and positive mean before and after the change, respectively.

C. Experiment 3: Performance of the SC-MA integrity metric.

Finally, we do the same as in the previous experiment but comparing with the single-correlation metric in (18) and the method suggested in [7]. Here, we also use a precorrelation bandwidth of 4 MHz, the same SMR and multipath values as in the previous experiment, and low C/N_0 scenarios are simulated. Fig. 8 shows the CUSUM performance of the method in [12] and the one developed in this work, fixing $C/N_0 = 26$ dB-Hz.

The upper plot of Fig. 8 represents the detection delay with respect to the set threshold, showing lower values for the complex distribution (i.e proposed method in (19)) than for the real one (i.e method in [12]). However, the lower plot shows how the FAR is lower for the complex than for the real case. Then, to fix a similar FAR in both methods, the threshold must be increased in the complex with respect the real case. This leads to an increase in the detection delay, with respect to that achieved when using the same thresholds in both methods.

Taking a look at the lower plot of Fig. 8, it can be seen how for a FAR of around 40 ms, the real case threshold must be fixed to 4 while for the complex case, it must be fixed to almost 14. With these thresholds, and coming back to the upper plot of Fig.

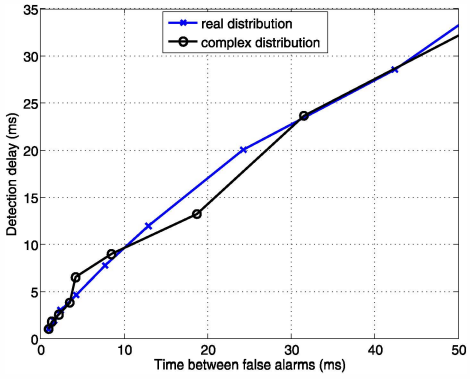

Fig. 9. Delay detection vs false alarm for the real and complex distribution assumption.

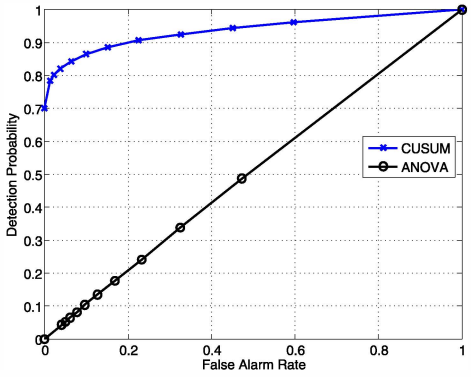

Fig. 10. Simulated ROC comparison between the proposed single-correlation method and the ANOVA test.

8, it can be proved that a similar detection delay is achieved in both cases. Therefore, we have the same performance for both methods, but needing an higher threshold in the complex case than in the real one. This is intuitive because in the imaginary case, the method needs more time to have an accurate estimation to be used in the GLR CUSUM. In turn, this more accurate estimates will help us in reducing the false alarm rate.

Fig. 9 shows the CUSUM performance as a function of the detection delay with respect the FAR for both methods, corroborating the same performance for both approaches. This is clear because the real and imaginary part of a complex Gaussian random variable, are distributed as real Gaussian variables. Thus, to evaluate them separately is the same as to evaluate them at the same time but using the complex distribution (i.e. both models are equivalents).

In order to compare the single-correlation method with some other already available in the literature, we compare it with that used in [7]. The latter is based on the statistical analysis of variance (ANOVA) procedure, which is applied to the received signal after removing the LOS contribution (i.e. $\mathbf{z}(k)$ used in (18)). In this case, the ANOVA method needs at least to use two samples (i.e. two integration periods). To do a fair comparison between ANOVA and our single-correlation procedure, we can use in our technique a PDI time being twice the one used in ANOVA. Thereby, both methods will produce the same number of detections for a fixed time.

Hence, using the same procedure in experiment 2 to obtain detection and false alarm probabilities, and applying the previous assumptions to do a fair comparison, results in Fig. 10 are obtained, which show how our method outperforms ANOVA method. This is again consistent with the fact that the ANOVA is not designed to be used as a sequential detection method.

V. Conclusions

This paper adopts a quickest detection framework for multi-path/NLOS detection in multi-antenna GNSS receivers, with the aim of providing integrity in GNSS applications. Two receiver architectures have been considered, leading to two different detection metrics to be used in the CUSUM algorithm. For the multi-correlation architecture, the log-likelihood ratio is not completely known and thus an alternative metric with the same behavior as the LLR is needed (i.e. with a negative and positive mean, in the absence and presence of multipath, respectively). On the other hand, for the single-correlation architecture, we are forced to use the GLR CUSUM since the mean of the suggested metric in the presence of multipath is not known, leading to an increment of the computational burden compared with that of the multi-correlator method. Furthermore, remark that for multi-correlation architectures both MC-MA and SC-MA metrics can be used. However, comparing Fig. 10 and the lower plot of Fig. 7 can be inferred the outperforming of MC-MA, being the best choice in multi-correlation architectures. Whereas for single-correlation architectures only the SC-MA method can be applied since the MC-MA can't be achieved. Numerical results of these techniques show the potential interest of them in practical applications involving GNSS signal integrity real-time monitoring, since the proposed methods outperform current classical multipath detectors.

References

[1] B. W. Parkinson and J. J. Spilker, *Global Positioning System: Theory and Applications vol. 2*. Aiaa, 1996, vol. 2.

[2] J. Cosmen-Schortmann, M. Azaola-Saenz *et al.*, "Integrity in urban and road environments and its use in liability critical applications," in *IEEE/ION Pos., Loc. and Nav. Sympos.*, 2008, pp. 972–983.

[3] G. Seco-Granados, J. A. Lopez-Salcedo *et al.*, "Challenges in indoor global navigation satellite systems: Unveiling its core features in signal processing," *IEEE Sig. Process. Mag.*, vol. 29, no. 2, pp. 108–131, 2012.

[4] H. K. Lee, J. G. Lee *et al.*, "GPS multipath detection based on sequence of successive-time double-differences," *IEEE Sig. Process. Lett.*, vol. 11, no. 3, pp. 316–319, 2004.

[5] C. Pinana-Diaz, Toledo-Moreo *et al.*, "GPS multipath detection and exclusion with elevation-enhanced maps," in *14th Int. IEEE Conf. on Intell. transp. syst. (ITSC)*, 2011, pp. 19–24.

[6] M. Obst, S. Bauer *et al.*, "Urban multipath detection and mitigation with dynamic 3D maps for reliable land vehicle localization," in *IEEE/ION Pos. Loc. and Nav. Symp. (PLANS)*, 2012, pp. 685–691.

[7] M. Brenneman, Y. Morton *et al.*, "GPS multipath detection with ANOVA for adaptive arrays," *IEEE Aeros. and Electr. Syst., Trans. on*, vol. 46, no. 3, pp. 1171–1184, 2010.

[8] P. Closas and C. Fernández-Prades, "A statistical multipath detector for antenna array based GNSS receivers," *IEEE Wireless Comm., Trans. on*, vol. 10, no. 3, pp. 916–929, 2011.

[9] M. Basseville, I. V. Nikiforov *et al.*, *Detection of abrupt changes: theory and application*. Prentice Hall Englewood Cliffs, 1993, vol. 104.

[10] T. Oskiper and H. V. Poor, "Quickest detection of a random signal in background noise using a sensor array," *EURASIP J. Appl. Signal Process.*, vol. 2005, pp. 13–24, 2005.

[11] L. Lai, Y. Fan, and H. V. Poor, "Quickest detection in cognitive radio: A sequential change detection framework," in *IEEE Glob. Telecomm. Conf. (GLOBECOM)*, 2008, pp. 1–5.

[12] D. Egea, J. A. López-Salcedo, and G. Seco-Granados, "Interference and multipath sequential tests for signal integrity in multi-antenna GNSS receivers," in *IEEE 8th Sensor Array and Multichannel Signal Processing Workshop*, 2014, pp. 117–120.

[13] G. Seco-Granados *et al.*, "ML estimator and hybrid beamformer for multipath and interference mitigation in GNSS receivers," *Sig. Proc., IEEE Trans. on*, vol. 53, no. 3, pp. 1194–1208, 2005.